Title: A Novel and Active Catalyst Ag/ZnO for Oxidant-Free Dehydrogenation of Alcohols

Author: Mona Hosseini-Sarvari Tahereh Ataee-Kachouei Fatemeh Moeini

PII: S0025-5408(15)30040-4
DOI: http://dx.doi.org/doi:10.1016/j.materresbull.2015.07.019
Reference: MRB 8327

To appear in: *MRB*

Received date: 5-2-2014
Revised date: 30-6-2015
Accepted date: 16-7-2015

Please cite this article as: Mona Hosseini-Sarvari, Tahereh Ataee-Kachouei, Fatemeh Moeini, A Novel and Active Catalyst Ag/ZnO for Oxidant-Free Dehydrogenation of Alcohols, Materials Research Bulletin http://dx.doi.org/10.1016/j.materresbull.2015.07.019

A Novel and Active Catalyst Ag/ZnO for Oxidant-Free Dehydrogenation of Alcohols

Mona Hosseini-Sarvari,*Tahereh Ataee-Kachouei and Fatemeh Moeini,

Department of Chemistry, Shiraz University, Shiraz 71454, I. R. Iran.

To whom correspondence should be addressed:

Dr. Mona Hossseini-Sarvari

TEL: +98-711-6137169

FAX: +98-711-6460788

E-mail: hossaini@shirazu.ac.ir; monahosseini20@gmail.com

Graphical abstract

Synthesis and characterization of nano Ag/ZnO by varying loading of Ag on ZnO support using a new and very simple method has been investigated.

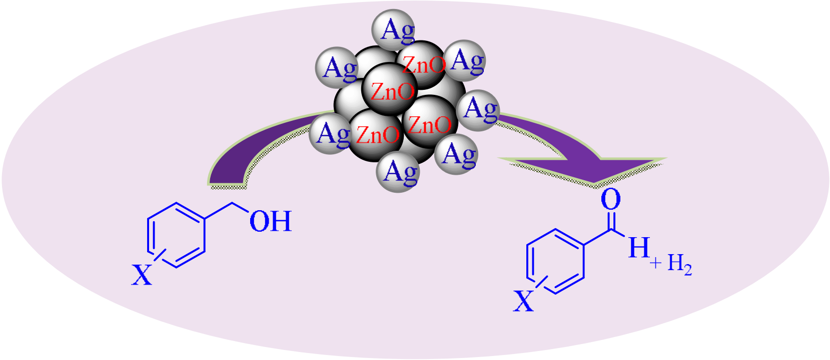

Highlights

- Synthesis and characterization of small amount of Ag supported on ZnO
- Nano Ag/ZnO as highly efficient heterogeneous catalyst
- Nano Ag/ZnO for oxidant-free oxidation
- nano Ag/ZnO has been confirmed by various methods

Abstract

Nano Ag/ZnO catalysts were prepared by varying load of Ag on ZnO support using a new and very simple method. The structure of nano Ag/ZnO has been confirmed by various techniques. The Ag/ZnO with 7.4×10^{-5} mol% of Ag has pore size distribution about 2.74 nm and this nano Ag/ZnO is found to be the best catalyst for oxidation of primary and secondary benzyl alcohols into corresponding aldehydes and ketones in oxidant-free at the atmospheric pressure. The influence of various parameters such as: solvent, base, temperature, time of reaction, and etc. has been systematically studied on nano Ag/ZnO catalyst.

Keywords: Nano Ag/ZnO; heterogeneous catalyst; oxidation; oxidant-free oxidation

1. Introduction

Oxidation of alcohols to carbonyl compounds is one of the important transformations in organic synthesis, since the oxidation products are essential intermediates in the manufacture of high-value fine chemicals, agrochemicals, pharmaceutical and high-tonnage commodity chemicals [1,2]. To accomplish economical and environmental acceptability, much effort has been applied to the oxidation of alcohols with environmentally friendly oxidants such as oxygen (O_2) or hydrogen peroxides [3], because of the necessity replacing stoichiometries reactions involving toxic oxidants such as chromium and manganese salts and other classical procedures [4]. Even though in many of these aerobic oxidation methods, homogeneous systems were used and share common disadvantages because work up, and catalyst reuse is difficult.

In fact, from the safety and environmental issues, using more atom-efficient catalyst systems, which do not use molecular oxygen or air for dehydrogenation of alcohols to carbonyl compounds and molecular hydrogen would be ideal. So, using an oxidant-free methodology is particularly interesting both from an environmental and a practical point of view because *i*) the formation of H_2O, as a byproduct is eliminated, which often tedious purification of products from the aqueous reaction mixture is needed, *ii*) it is useful for alcohols bearing functional groups which are sensitive to O_2, *iii*) H_2 is produced, which it is an attractive feedstock for energy generation, and *iv*) it is avoided possible over oxidation of the substrate to carboxylic acids. Therefore, a series of transition metal catalysts (Ru, Ir, Au, Ag, Pt, Cu and etc.) have been developed for oxidant-free dehydrogenation of alcohols. Homogeneous and heterogeneous Ru [5-9] and Ir [10–13] catalysts have been reported for dehydrogenation of alcohols, but they variously suffer from drawbacks such as difficulties in catalyst reuse, the requirement of acid or base additives, difficulties in catalyst synthesis, manipulation, high cost, and low activity for the primary alcohol dehydration. Heterogeneous Pt [14,15], Au [16], Cu [17,18], Co [19], Ni [20], and Ag [21,22] catalysts were also reported to be effective. Among them, there are a few reports on using Ag catalysts for the oxidant-free dehydrogenation of alcohols. Although these supported silver nanoparticles are attractive as the most active catalyst for this reaction, but they suffer from drawbacks. In these few methods before using the catalyst it should be treated under H_2 in order to reduce Ag^I to Ag^0, the amount of silver used as catalysts are 0.005 and 1-10 mole%, respectively, and the reactions were placed under Ar or N_2 flows.

ZnO, as one of the most semiconductor oxide nanostructures is attracting significant attention because they can act as potential candidates for applications in energy generators, sensors, lasers, optoelectronics and light-emitting diodes [23-27]. In particular, nano zinc oxide has been proven to exhibit better photocatalytic proficiency for the degradation of some organic compounds than that of the TiO_2, which is currently the most extensively-studied photocatalysis. ZnO is also biodegradable, nontoxic and biocompatible for environmental applications. Recent researches revealed that modification with noble metals, such as Au, Ag, or Pt, is an effective way to prohibit the recombination of charge carriers and to raise the photocatalytic performance of ZnO photocatalyst for degrading toxic organic pollutants. Especially, Ag/ZnO nanostructures with various morphologies have been obtained with different synthesis strategies [28-31].

Being an eco-friendly and high performance catalyst for the oxidation of alcohols, herein, in this study, the catalysts Ag/ZnO was prepared by a simple method, and it was used as an active and efficient catalyst for the oxidation of a wide range of benzylic alcohols for the first time.

2. Experimental

2.1. Preparation of nano Ag/ZnO

All the reagents, including, Zinc nitrate ($Zn(NO_3)_2.6H_2O$), silver nitrate ($AgNO_3$) and urea were all obtained from Fluka or Merck and used as received without further purification. The synthesis of nano

Ag/ZnO is as follows: $Zn(NO_3)_2.6H_2O$, $AgNO_3$ and $CO(NH_2)_2$ were dissolved in a minimum quantity of deionized water to form a transparent solution. In practice, the addition of 10% more than the stociometric amount of urea was preferred. The mixture was refluxed for 6 h at 100°C. The product was centrifuged and washed with deionized water and absolute ethanol. Then the Ag/ZnO nano powders were allowed to dry at 80°C in an oven. Then the nanoparticles were annealed at 500 °C for 3 h in high temperature furnace. According to this method, four kinds of nano Ag/ZnO were prepared in more than 95% isolated yields which the molar ratio of $AgNO_3$: $Zn(NO_3)_2.6H_2O$ was 1:1, 1:2, 1:4, and 1:8, respectively.

2.2. General procedure for the dehydrogenation of benzylic alcohols using Ag/ZnO nanoparticles

A mixture of alcohol (1 mmol), KOH (1 mmol), and 0.005g Ag/ZnO nanoparticles (2) (containing $8x10^{-5}$ g Ag) in toluene (2 mL) was stirred at 100 ºC for the appropriate time. The reaction was monitored by thin layer chromatography (TLC) or GC. After completion of the reaction, the reaction mixture was diluted with EtOAc and centrifuged to remove the catalyst. The filtrate was extracted with water, the organic layer dried over $CaCl_2$ and evaporated under reduced pressure. The resulting product was purified by column chromatography on silica-gel to afford the pure product. All compounds are known and were characterized by comparison of their physical and spectroscopic data with the already described in the literature.

3. Results and Discussion

3.1. Catalyst preparation

Nano Ag/ZnO catalyst was prepared in high yield by precipitation method (more than 95% isolated yield). Based on related literature [32-37], a possible mechanism is proposed, as schematically in equations 1-9.

$$CO(NH_2)_2 + 3\ H_2O \longrightarrow 2NH_4^+ + CO_2 + 2OH^- \tag{1}$$

$$Zn(NO_3)_2 .6\ H_2O + H_2O \longrightarrow Zn^{2+} + 2NO_3^- \tag{2}$$

$$AgNO_3 + H_2O \longrightarrow Ag^+ + NO_3^- \tag{3}$$

$$Zn^{2+} + 2OH^- \longrightarrow Zn(OH)_2 \downarrow \tag{4}$$

$$Ag^+ + OH^- \longrightarrow AgOH \downarrow \tag{5}$$

$$Zn(OH)_2 + 2OH^- \longrightarrow Zn(OH)_4^{2-} \tag{6}$$

$$AgOH + OH^- \longrightarrow Ag(OH)_2^- \tag{7}$$

$$Zn(OH)_4^{2-} + 2Ag(OH)_2^- \longrightarrow Ag_2O / ZnO + 2H_2O + 4OH^- \tag{8}$$

$$Ag_2O / ZnO + NH_4^+ \longrightarrow Ag/ZnO \tag{9}$$

At first, $Zn(NO_3)_2$ and $AgNO_3$ were reacted with H_2O and corresponding Zn^{2+} and Ag^+ ions were formed (eq. 2, 3). By the addition of urea, $Zn(OH)_2$ and AgOH were formed (eq. 4,5). When the amount of urea increased (addition of 10%) more than the stoichiometric amount, $Zn(OH)_2$and AgOH will be gradually dissolved into $Zn(OH)_4^{2-}$ and $Ag(OH)_2^-$, respectively (eq. 6,7). Under the alkaline thermal condition, intermolecular dehydrolysis between $Zn(OH)_4^{2-}$ and $Ag(OH)_2^-$ may occur, and Ag_2O/ZnO formed (eq. 8). Urea here plays a dual role, acting not only as a co-solvent but also as a reducing agent to reduce Ag^+ into Ag. Finally, nano Ag/ZnO would be produced.

According to this method, four kinds of nano Ag/ZnO were prepared. The content of Ag in nano Ag/ZnO was varied from 10^{-4} g (9.3×10^{-5} mol%) (Ag/ZnO (1)), $8x10^{-5}$ g (7.4×10^{-5} mol%) (Ag /ZnO (2)), $4x10^{-5}$ g (3.6×10^{-5} mol%) (Ag/ZnO (3)), and $3.5x10^{-5}$ g (3.3×10^{-5} mol%) (Ag/ZnO (4)), which the molar ratio of $AgNO_3$: $Zn(NO_3)_2.6H_2O$ was 1:1, 1:2, 1:4, and 1:8, respectively. The physical appearance of these catalysts can be seen in Figure 1. The natural color of ZnO is white. By increasing the amount of Ag doped on ZnO, the colors of the catalysts were changed from white to dark-brown.

3.2. Characterization of the catalyst

X-ray diffraction (XRD) patterns of nano Ag/ZnO with various amounts of Ag doped on ZnO, nano Ag and nano ZnO are shown in Figure 2. The diffraction peaks could be categorized into two sets. Those marked with "#" are the diffraction peaks at $2\theta = 32^o$, 34^o, and 36^o and are indexed to (100), (002), and (101) diffractions of hexagonal structured ZnO (wurtzite) (JCPD No. 36-1451) respectively, while the others marked with "*" and located at $2\theta = 38^o$ and 44^o are characteristic to (111) and (200) diffractions of FCC structured Ag (JCPDS No. 04-0783), respectively. The sharp diffraction peaks indicate that the nano Ag/ZnO is highly crystallized. Besides, the diffraction peaks corresponding to silver oxide species, for example Ag_2O at 32.97◦ are not detected, so it can be concluded that there is no silver oxide species in the samples as well [38]. Furthermore, from (a) to (f) a consistent decrease in the intensity of silver peaks can be noted with the decrease in concentration of Ag from 9.3×10^{-5}, 7.4×10^{-5}, 3.6×10^{-5} and 3.3×10^{-5} mol%, respectively. Additionally, the average sizes of the ZnO and Ag nanoparticles, calculated by the *Scherrer* formula [39] applied to the major peaks ($2\theta = 34^o$ for ZnO) were estimated to be approximately 36.28, 36.02, 39.6, 30.13 and 65.04 nm for Ag/ZnO (**1**), Ag/ZnO (**2**), Ag/ZnO (**3**), Ag/ZnO (**4**) and nano ZnO, respectively, and ($2\theta = 38^o$ for Ag) were estimated to be approximately 45.83 nm, 43.79 nm, 53.31 nm, 31.55 nm and 25.57 nm for Ag/ZnO (**1**), Ag/ZnO (**2**), Ag/ZnO (**3**), Ag/ZnO (**4**) and nano Ag, respectively. With the obtained XRD results, indicated that the present catalyst (Ag/ZnO) shows the presence of Ag only, and not any peaks for silver oxides (AgO, or Ag_2O) were observed. In subsequent paragraphs we will prove this by XPS method.By comparing the XRD pattern of pure hexagonal ZnO and nano Ag/ZnO (Figure 3), there is a shift in the peak position of ZnO for the prepared Ag/ZnO samples (~0.15^o). Generally this shift in peak position value is observed when a doping element having larger ionic radius than Zn^{2+} is replaced at the substitutional sites of the ZnO crystal lattice. Zn^{2+} ion (0.71 ^{o}A) has lower ionic size than Ag^+ (1.22 ^{o}A). So, this shift toward the XRD peak position can suggest that Ag ion has occupied the interstitial sites of ZnO [40].

The surface structure of the Ag/ZnO sample with an Ag content of 7.4×10^{-5} % was investigated by using X-ray photoelectron spectroscopy (XPS) analysis, and the results are shown in Figure 4. All of the peaks in the curve can be ascribed to Ag, Zn, O, and C elements, while C 1s at 285 eV is due to the hydrocarbon from the XPS instrument itself [41]. Clearly all the peaks are ascribed to Zn, O, and Ag, and no peaks characteristics of impurities are observed. Figure 4b, shows the Zn 2p XPS spectra of the catalyst. Because of strong spin-orbit coupling, the Zn 2p peak split into Zn $2p_{3/2}$ and Zn $2p_{1/2}$ with a doublet peak energy separation of ~23 eV. The peak positions at 1022.8 and 1045.7 eV corresponds to the Zn 2p3/2, and Zn 2p1/2, respectively, which confirm that the Zn in the catalyst mainly exists for the form of Zn^{2+} [42]. Figure 4c provides the XPS spectra of Ag. The Ag $3d_{5/2}$ and $3d_{3/2}$ peaks appear at a binding energy of 367.5 and 373.1 eV, respectively. Here, interestingly, the peaks of Ag in our work were found to shift to the lower binding energy compared with the standards value (about 368.2, and 374.1 eV). This confirms the interaction between Ag and ZnO nano crystals. When the Ag and ZnO nanoparticles attach together, they adjust the position of their corresponding Fermi energy levels to the same value. Thus, there are many free electrons above the new Fermi level of metallic Ag nanoparticles. Because the conduction band (CB) of ZnO nanoparticles is vacant, the free electrons could tunnel into the CB, resulting in the higher valence of Ag [43,44]. This is in consistent with the results from XRD. Figure 4d shows the O 1s peaks of Ag/ZnO catalyst. The O 1s peak can be divided into two peaks at about 530 and 532 eV, corresponding to the lattice oxygen and surface hydroxyl oxygen, respectively.

The Brunauer-Emmett-Teller analysis (BET) gas adsorption–desorption measurements of nano Ag/ZnO (**2**) catalyst synthesized in this work is measured and the results are shown in Table 1.

The morphology of nano Ag/ZnO (**2**) obtained from transmission electron microscopy (TEM) analysis was displayed in Figure 5. The size of Ag/ZnO nanoparticle that was seen from TEM image was about in the range of 34 nm.

3.3. Catalytic activity of nano Ag/ZnO for oxidation of benzyl alcohols

After successful synthesis and fully characterize of nano Ag/ZnO, we examined its catalytic activity for oxidant-free oxidation of alcohols (Scheme 1).

Our first attempt in this study was to find a proper and efficient optimum reaction conditions. So, 3-methoxy benzylalcohol was chosen as a model compound and various parameters such as bases, solvents, temperature, the amount of catalyst, and different Ag loading were studied. The results are described in Tables 2-4.

According to Table 2, nano Ag/ZnO (**2**) was chosen as an effective catalyst for the oxidant-free oxidation. According to these results, Ag/ZnO (**1**) (9.3×10^{-5}mol% Ag) and Ag/ZnO (**2**) (7.4×10^{-5}mol% Ag (entries 1 and 6) showed the same yields, but we chose nano Ag/ZnO (**2**) because of the lower amount of Ag loading on ZnO. From the results obtained from Tables 2-4, we can conclude that when 3-methoxy benzyl alcohol (1 mmol) was treated in the presence of nano Ag/ZnO (**2**) (0.005 g), KOH (1 mmol) at 100 ^{o}C in toluene (2 mL) for 6 h, 3-methoxy benzaldehyde was produced in 80% isolated yield with 99% selectivity.

Thus, we chose Ag/ZnO (**2**) as the standard catalyst and the scope and generality was explored next. The results are summarized in Table 5. According to Table 5, various substituted alcohols bearing electron-donating and withdrawing groups were examined; substituted alcohols with electron-donating groups had more yield than that of withdrawing groups. In addition, *p*-substituted alcohols with electron-donating groups had better yields in comparing with the others. According to Table 5, the lowest yield was observed for 2-nitrobenzaldehydes because of the *o*-substituted and a strong electron withdrawing group. It is important to note that secondary alcohols were also tolerated with good yields (entries 13, 17, 18). In addition, heterocyclic alcohols, such as 2-thiophenemethanol, and 2-pyridinemethanol (entries 15, 16), were oxidized to the corresponding aldehydes in high yields. No oxidation was observed with S and N hetero atoms.

The heterogeneity of the catalyst was evaluated to study whether the reaction using solid catalysts or was catalyzed by nano Ag/ZnO species in the liquid phase. To address this issue, two separate experiments were conducted with 3-methoxy benzyl alcohol. In the first experiment, the reaction was terminated after two hours; at this juncture, the catalyst was separated from the reaction mixture and the reaction was continued with the filtrate for an additional three hours. In the second experiment, the reaction was terminated after two hours. In both cases, the desired product was obtained in the same yield (50%). Ag was not detected in the filtrate in either experiment by ICP analyzer. These studies demonstrate that only the Ag support on ZnO during the reaction is active, and the reaction proceeds on the heterogeneous surface. We also confirmed that no leaching of Ag from the Ag/ZnO catalyst occurred during the dehydrogenation of 3-methoxy benzyl alcohol. No Ag can be detected in the filtrate after the reaction.

A proposed mechanism for the role of nano Ag/ZnO as catalyst is shown in Scheme 2. The first step of the reaction is proton abstraction from the alcohol by KOH to yield an alkoxide group. The ZnO has Lewis acid sites (Zn^{+2}) and also Lewis basic sites (O^{2-}) [45]. The Lewis acid site of ZnO is coordinated to the oxygen of the alkoxide group, and also a hydrogen-bonded with water molecules, which generated from the proton abstraction by KOH. In view of the role of the silver, we propose that Ag atoms play an important role in the a-C-H activation step. So, in the next step, alkoxide species at the interface between a silver and ZnO undergo hydride abstraction to yield hydride species on the Ag and aldehydes *via* a transition state with a positive charge at the α-carbon atom. Then, a hydride ion on the Ag reacts with the water molecule, which absorbed on Lewis acid sites of ZnO, to yield H_2. Bronsted acidities of the hydrogen atoms of absorbed water on the surface of ZnO are increased because of the Lewis acid sites of ZnO. This acid-base mechanism can facilities the release of the H_2.

A comparison of the present catalyst, using nano Ag/ZnO, with some of previously known Ag catalysts is collected in Table 6 to demonstrate that the present catalyst is indeed superior to several of the other protocols. According to Table 5, the selective oxidation of benzylalcohol to benzaldehyde is completed in 8 h at 120 8C in 98% isolated yield by using Ag/ZnO (2). Most of the other Ag catalysts listed either take a longer reaction time for completion, higher reaction temperature or require to use under inert atmosphere with generally reduced isolated yields. Thus, nano Ag/ZnO was found to be the better choice for this reaction.

Finally, The catalyst Ag/ZnO after reaction was characterized by XRD and the patterns images is shown in Figure 6.

4. Conclusions

In conclusion, the ZnO supported small amount of silver nano catalyst prepared by a very simple and low cost method with small particles sizes around 36 nm and characterized in terms of its structural aspects. This nano Ag/ZnO acts as an efficient heterogeneous catalyst for oxidant-free dehydrogenation of benzyl alcohols in a very mild reaction conditions without the use of any Ar or N_2 flow. The Ag/ZnO afforded high yields of the corresponding carbonyl compounds with co-production of equivalent molar amounts of H_2.

Acknowledgements

We gratefully acknowledge the support of this work by the Shiraz University Research Council.

References

[1] R. A. Sheldon, H. Bekkum, Fine chemical through heterogeneous catalysis (Chapter 9), Wiley-VCH, Weinheim, 2001.

[2] H. A. Wittcoff, B. G. Reuben, J. S. Plotkin, Industrial organic chemical, Wiley, New Jersey, 2004.

[3] a) T. Ishida, M. Nagaoka, T. Akita, M. Haruta, Chem. Eur. J.0, 14 (2008) 8456-8460; b) K. Mori, T. Hara, T. Mizugaki, K. Ebitani, K. Kaneda, J. Am. Chem. Soc. 126 (2004) 10657-10666; c) T. Mallat, A. Baiker, Chem. Rev. 104 (2004) 3037-3058; d)L. Liu, B. B. Wayland, X. Fu, Chem. Commun. 46 (2010) 6353-6355; e) T.Yasu-eda, S. Kitamura, N. Ikenaga, T. Miyake, T. Suzuki, J. Mol. Catal. A: Chem. 323 (2010) 7-15; f) P. Muthupandi, G. Sekar, Tetrahedron Lett. 52 (2011) 692-695; g) K. Kaizuka, H. Miyamura, S. Kabayashi, J. Am. Chem. Soc. 132 (2010) 15096-15098; h) C. X. Miao, J.Q.Wang, B. Yu, W.G. Cheng, J. Sun, S. Chanfreu, L.N. He, S.J. Zhang, Chem. Commun. 47 (2011) 2697-2699; i) G. Urgoitia, R. SanMartin, M.T. Herrero, E. Dom´ınguez, Green Chem. 13 (2011) 2161-2166; J) N. Dimitratos, J.A. Lopez-Sanchez, G.J. Hutchings, Chem. Sci. 3 (2012) 20-44; k) R. J. Angelici, Catal. Sci. Technol. 3 (2013) 279-296; (l) S.E. Davis, M.S. Ide, R.J. Davis Green Chem. 15 (2013) 17-45.

[4] a) M. Hunsen, Tetrahedron Lett. 46 (2005) 1651-1653; b) C. Wiles, P. Watts, S.J. Haswell, Tetrahedron Lett. 47 (2006) 5261-5264; c) M.Z. Kassaee, S.Z. Sayyed-Alangi, H. Sajjadi-Ghotbabadi, Molecules 9 (2004) 825-829; d) K. Krohn, I. Vinke, H. Adam, J. Org. Chem. 61

(1996) 1467-1472; e) S. Azizian, A. Eftekhari-Bafrooei, H. Bashiri, Kinet. Catal. 51 (2010) 244-249; f) M. M. Najafpour, M. Halynska, M. Aminim, S.H. Kazemi, T. Lis, M. Bagherzadeh, Polyhedron 29 (2010) 2837-2843; g) M.S. Yusubov, A. A. Zagulyaeva, V.V. Zhadankin, Chem. Eur. J. 15 (2009) 11091-11094.

[5] J. Zhang, M. Gandelman, L.J.W. Shimon, H. Rozenberg, D. Milstein, Organometallics 23 (2004) 4026-4033.

[6] M. Nielsen, A. Kammer, D. Cozzula, H. Junge, S. Gladiali, M. Beller, Angew. Chem. Int. Ed. 50 (2011) 9593-9597.

[7] J.H. Choi, N. Kim, Y.J. Shin, J.H. Park, J. Park, Tetrahedron Lett. 45 (2004) 4607-4610.

[8] W.H. Kim, I.S. Park, J. Park, Org. Lett. 8 (2006) 2543-2545.

[9] B. Feng, C. Chen, H. Yang, X. Zhao, L. Hua, Y. Yu, T. Cao, Y. Shi, Z. Hou, Adv. Synth. Catal. 354 (2012) 1559-1565.

[10] K.-I. Fujita, N. Tanino, R. Yamaguchi, Org. Lett. 9 (2007) 109-111.

[11] R. Kawahara, K.-I. Fujita, R. Yamaguchi, Angew. Chem. Int. Ed. 51 (2012) 12790-12794.

[12] S. Musa, I. Shaposhnikov, S. Cohen, D. Gelman, Angew. Chem. Int. Ed. 50 (2011) 3533-3537.

[13] K. Oded, S. Musa, D. Gelman, J. Blum, Catal. Commun. 20 (2012) 68-70.

[14] M. Yamashita, F. Dai, M. Suzuki, Y. Saito, Bull. Chem. Soc. Jpn. 64 (1991) 628-634.

[15] Y. Ando, M. Yamashita, Y. Saito, Bull. Chem. Soc. Jpn. 76 (2003) 2045-2049.

[16] a) W.-H. Fang, J.-S. Chen, Q.-H. Zhang, W.-P. Deng, Y. Wang, Chem. Eur. J. 17 (2011) 1247-1256; b) W. Fang, Q. Zhang, J. Chen, W. Deng Y. Wang, Chem. Commun. 46 (2010) 1547-1549.

[17] T. Mitsudome, Y. Mikami, K. Ebata, T. Mizugaki, K. Jitsukawa, K. Kaneda, Chem.Commun. 44 (2008) 4804-4806.

[18] R.K. Marella, C.K.P. Neeli, S.R.R. Kamaraju, D.R. Burri, Catal. Sci. Technol. 2 (2012) 1833-1838.

[19] K. Shimizu, K. Kon, M. Seto, K. Shimura, H. Yamazaki, J. N. Kondo, Green Chem. 15 (2013) 418-424.

[20] K. Shimizu, K. Kon, M. Seto, K. Shimura, S.S.M.A. Hakim, J. Catal. 300 (2013) 242-249.

[21] T. Mitsudome, Y. Mikami, H. Funai, T. Mizugaki, K. Jitsukawa, K. Kaneda, Angew. Chem. Int. Ed. 47 (2008) 138-141.

[22] K. Shimizu, K. Sugino, K. Sawabe, A. Satsuma, Chem. Eur. J. 15 (2009) 2341-2351.

[23] Y. M. Zhang, D. Lan, Y. R. Wang, H. Cao, H. Jiang, Physica E. 43 (2011) 1219-1223.

[24] J. Demel, J. Plestil, P. Bezdicka, P. Janda, M. Klementova, K. Lang, J. Phys. Chem. C. 115 (2011) 24702-24706.

[25] Z. L. Wang, ACS Nano 2 (2008) 1987-1992.

[26] S.H.Ko, D. Lee, H.W. Kang, K.H. Nam, J.Y. Yeo, S.J. Hong, C.P. Grigoropoulos, H.J. Sung, Nano Lett. 11 (2011) 666-671.

[27] J.H. Tian, J. Hu, S.S. Li, F. Zhang, J. Liu, J. Shi, X. Li, Z. Q. Tian, Y. Chen, Nanotechnology 22 (2011) 1-9.

[28] D. Lin, H. Wu, R. Zhang, W. Pan, Chem. Mater. 21 (2009) 3479-3484.

[29] Y.C. Yang, F. Pan, Q. Liu, M. Liu, F. Zeng, Nano Lett. 9 (2009) 1636-1643.

[30] X.M. Feng, G. Q. Hu, J. Q. Hu, Nanoscale 3 (2011) 2099-2117.

[31] a) G.X. Zhu, Y.J. Liu, H. Xu, Y. Chen, X.P. Shen, Z. Xu, Cryst. Eng. Comm. 14 (2012) 719-725; b) B. Subash, B. Krishnakumar, R. Velmurugan, M. Swaminathan, M. Shanthi, Catal. Sci. Technol. 2 (2012) 2319-2326.

[32] J. Xie, Q. Wu, Mater. Lett. 64 (2010) 389-392.

[33] Sh. Gao, X. Jia, Sh. Yang, Zh. Li, K. Jiang, J. solid state 184 (2011) 764-769.

[34] X.-Y. Ye, Y.–M. Zhou, Y.–Q. Sun, J. Chen, Z.–Q. Wang, J. Nanopart. Res. 11 (2009) 1159-1166.

[35] Y. Zheng, Ch. Chen, Y. Zhan, X. Lin, Q. Zheng, K. Wei, J. Zhu, J. Phys. Chem. C. 112 (2008) 10773-10777.

[36] G. Zhou, J. Deng, Mater. Sci. Semicond. Process. 10 (2007) 90-96.

[37] D. Sahu, B. S. Acharya, A. K. Panda, Ultrason. Sonochem. 18 (2011) 601-607.

[38] S. Seki, T. Sekizawa, K. Haga, T. Sato, M. Takeda, Y. Seki, Y. Sawada, J. Vac. Sci. Technol. B. 28 (2010) 188-193.

[39] N.N. Greenwood, A. Earnshaw, Chemistry of the Elements (2nd ed.), Oxford: Butterworth-Heinemann, 1997.

[40] B.D. Ahn, H.S. Kang, J.H. Kim, G.H. Kim, H.W. Chang, S.Y. Lee, J. Appl. Phys. 100 (2006) 093701.

[41] J.G. Yu, J.F. Xiong, B. Cheng, S.W. Liu, Appl. Catal. B 60 (2005) 211-221.

[42] NIST X-ray Photoelectron Spectroscopy Database: http://srdata.nist.gov/xps/.

[43] F. Moudler, W. F. Stickle, P. E. Sobol, K. D. Bomben, Handbook of X-ray Photoelectron Spectroscopy Perkin-Elmer, MN.

[44] L. Jing, Z. Xu, J. Shang, X. Sun, W. Cai, H. Guo, Mater. Sci. Eng. A. 332 (2002) 356-361.

[45] M. Hosseini-Sarvari, M. Tavakolian, Appl. Catal. A. 441 (2012) 65-71.

[46] T. Mitsudome, Y. Mikami, H. Funai, T. Mizugaki, K. Jitsukawa, K. Kaneda, Angew. Chem. 120 (2008) 144 –147.

[47] A. Bayat, M. Shakourian-Fard, N. Ehyaei, M. Mahmoodi Hashemi, RSC Adv. 5 (2015) 22503–22509.

Table 1. Results of BET surface area measurements for Ag/ZnO (**2**)

Surface area	BET surface area (m^2/g)	4.204
	BJH adsorption cumulative surface area of pores (m^2/g)	4.859
Pore volume	Single point adsorption total pore volume of pores (cm^3/g)	0.033
	BJH adsorption cumulative volume of pores (cm^3/g)	0.032
Pore size	Mean pore diameter (nm)	31.266
	Pore size distribution (nm)[a]	2.740

[a] The pore size distribution (PSD) is defined as the statistical distribution of the radius of the largest sphere that can be fitted inside a pore at a given point.

Table 2. Oxidation of 3-methoxy benzyl alcohol with different catalysts[a].

Entry	Catalyst	Time (h)	Yield (%)
1	Nano Ag/ZnO (**2**)[b]	5	80
2	Nano Ag	5	50
3	Nano ZnO	5	65
4	$AgNO_3$	5	40
5	$Zn(NO_3)_2$	5	10
6	Nano Ag/ZnO (**1**)[c]	4	80
7	Nano Ag/ZnO (**3**)[d]	6	75
8	Nano Ag/ZnO (**4**)[e]	6	70

[a] *Reaction condition*: 3-Methoxybenzyl alcohol (1 mmol), toluene (2 mL), KOH (1 mmol), catalyst (0.005 g), 100 ^{o}C. [b] The amount of Ag is 8×10^{-5} g. [c] 10^{-4} g . [d] 4×10^{-5} g and [e] $3.5 \times 10^{-}$ g.

Table 3. Base, solvent, and temperature optimization[a]

Entry	Base (1 mmol)	Solvent	Temp.(ºC)	Time (h)	Yield (%)
1	K_2CO_3	Toluene	100	10	20
2	Cs_2CO_3	Toluene	100	10	20
3	KOH	Toluene	100	6	80
4	$Ba(OH)_2$	Toluene	100	10	15
5	NaOH	Toluene	100	8	60
6	Na_2CO_3	Toluene	100	8	15
7	$Ca(OH)_2$	Toluene	100	10	15
8	KF	Toluene	100	8	10
9	Et_3N	Toluene	100	7	5
10	none	Toluene	100	9	15
11	K_3PO_4	Toluene	100	8	30
12	KOH	Toluene	100	6	80
13	KOH	DMF	100	7	15
14	KOH	DMSO	100	9	60
15	KOH	H_2O	100	6	0
16	KOH	EtOH	100	6	0
17	KOH	CH_3CN	100	6	15
18	KOH	none	100	8	50
19	KOH	THF	100	8	20
20	KOH	Toluene	100	6	80
21	KOH	Toluene	80	9	60

22	KOH	Toluene	60	11	40
23	KOH	Toluene	r.t.	10	10

[a] *Reaction conditions*: 3-Methoxy benzyl alcohol (1 mmol), nano Ag/ZnO (**2**) (0.005 g), base (1 mmol) solvent (2 mL)

Table 4. Amount of catalyst optimization[a]

Entry	nano Ag/ZnO (**2**) (g)	Time (h)	Yield (%)
1	0.05	6	80
2	0.025	6	80
3	0.0125	6	80
4	0.0063	5	80
5	0.005	5	80
6	0.004	5	70
7	0.003	5	50
8	0.002	5	50
9	0.001	5	50
10	none	5	50

[a] *Reaction conditions*: 3-Methoxy benzyl alcohol (1mmol), KOH (1 mmol), toluene (2 mL), 100 ^{o}C.

Table 5. Oxidation of benzyl alcohols using nano Ag/ZnO (**2**)[a]

Entry	Substrate	Product	Time (h)	Yield (%)
1	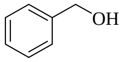	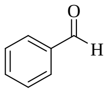	8	98
2	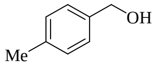	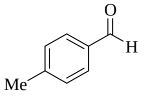	3	95
3	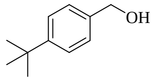	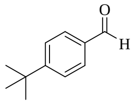	6	95
4	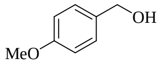	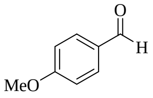	7	90
5	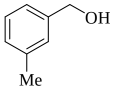	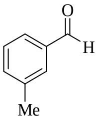	3	80
6	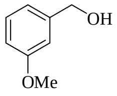	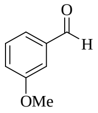	5 7	80 50[b]
7	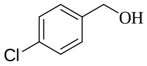	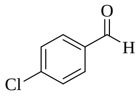	7	85
8	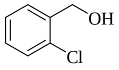	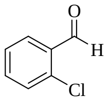	6	45
9	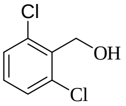	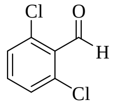	3	30
10	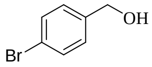	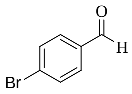	16	85
11	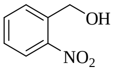	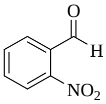	8	10

12	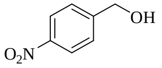	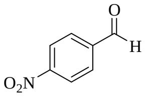	6.5	40
13	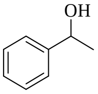	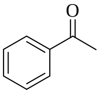	6	90
14	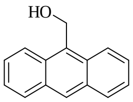	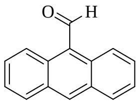	5	60
15	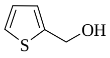	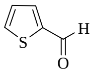	6	90
16	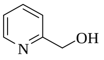	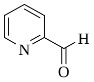	4	98
17	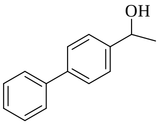	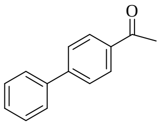	6	60
18	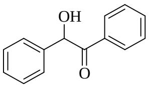	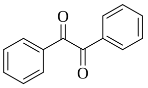	6	80

[a] *Reaction condition*: alcohol (1 mmol), toluene (2 mL), KOH (1 mmol), nano Ag/ZnO (**2**) (0.005g), 100 °C. [b] Large scale test.

Table 6. Oxidation of benzylalcohol catalyzed by various Ag catalysts.

Entry	Catalyst	Solvent	Temp. (^{o}C)	Time (h)	Yield (%)	Ref.
1	Ag/ZnO (2) (0.005 g)	Toluene (2 mL)	100	8	Isolated 98	Present work
2	Ag/HT(Hydrotalcites) (0.1 g)	p- Xylene (5 mL)	130/ Ar atmosphere	10	Conversion 99	[46]
3	Ag/Al_2O_3 (2 mol%)	Toluene (3 mL)	100	24	82	[22]
4	Fe_3O_4@SiO_2-Ag (0.5 mol%)	Toluene (3 mL)	Reflux/ N_2 atmosphere	24	Conversion 98	[47]

Figure captions

Figure 1. Physical appearance of various nanoAg/ZnO

Figure 2. The XRD patterns of the Ag/ZnO nanoparticles with various Ag doped on ZnO.

Figure 3. X-ray diffraction patterns of nano ZnO (red curve) and nano Ag/ZnO (**2**) (blue curve) for comparison.

Figure 4. XPS spectra of the sample with a Ag content of 7.391×10^{-5}mol %: (a) XPS full spectrum of the sample; (b) Zn 2p spectrum; (c) Ag 3d; (d) O 1s spectrum spectra.

Figure 5. Transmission electron microscopic (TEM) image of nano Ag/ZnO (**2**).

Figure 6. XRD pattern of catalyst a) before reaction b) after reaction

Scheme 1. Oxidant-free oxidation of benzyl alcohols using nano Ag/ZnO as catalyst

Scheme 2. A proposed mechanism

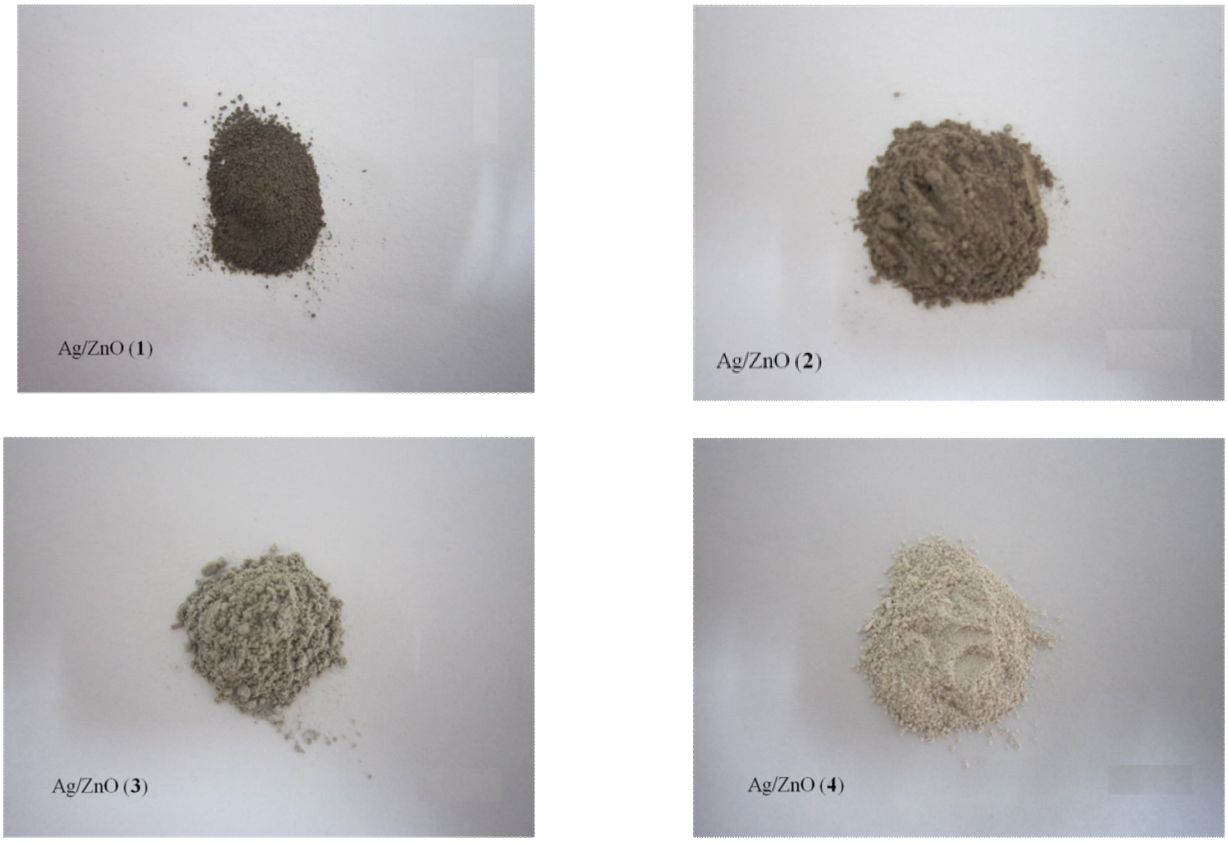

Figure 1.

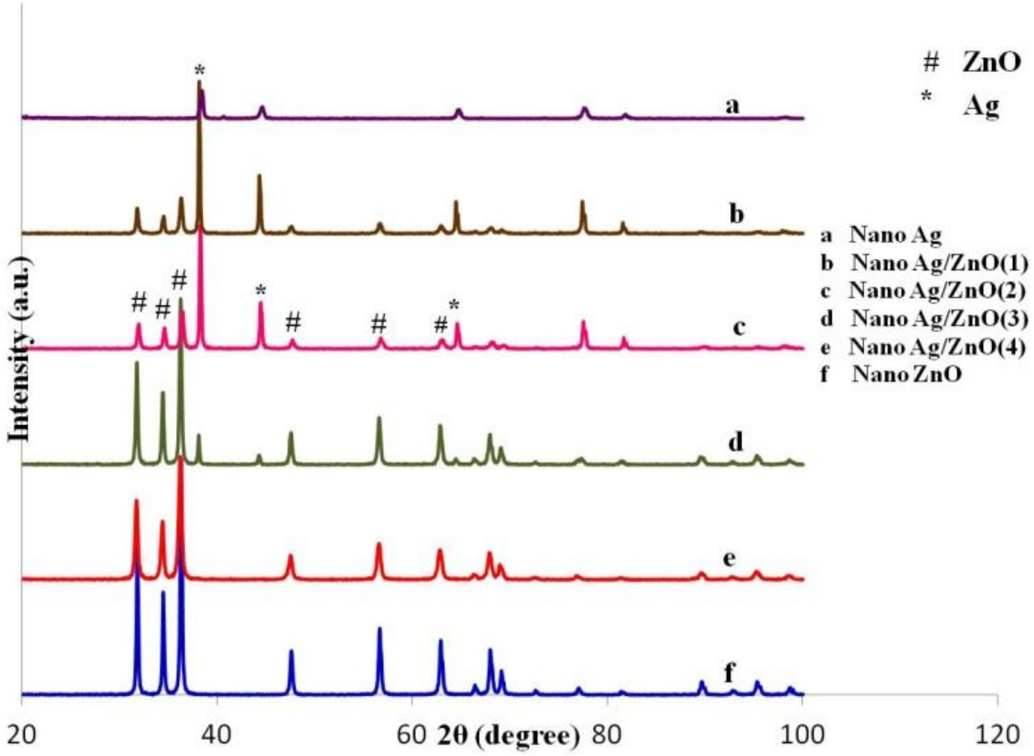
Intensity (a.u.)
2θ (degree)
20
40
60
80
100
120
ZnO
* Ag
a
b
c
d
e
f
a Nano Ag
b Nano Ag/ZnO(1)
c Nano Ag/ZnO(2)
d Nano Ag/ZnO(3)
e Nano Ag/ZnO(4)
f Nano ZnO
#
#
#
*
#
#
#
*
*

Figure 2.

`

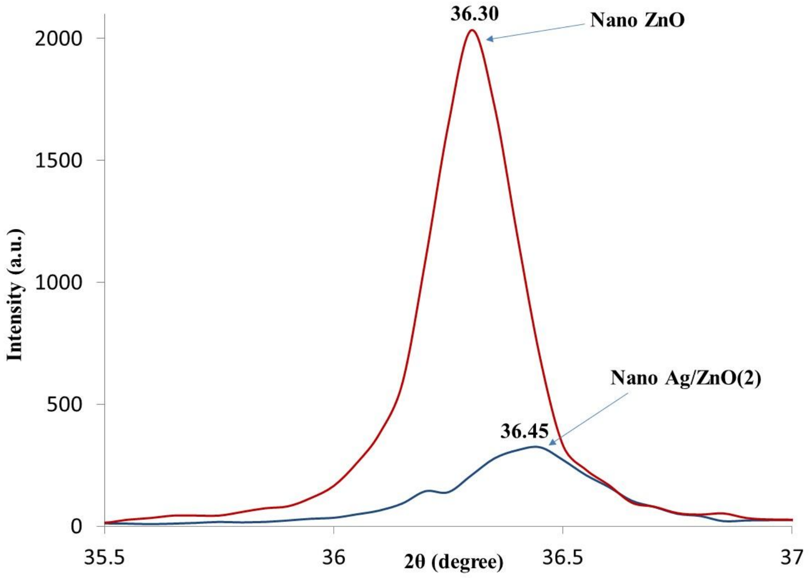
36.30
Nano ZnO
2000
1500
1000
500
0
Intensity (a.u.)
Nano Ag/ZnO(2)
36.45
35.5
36
2θ (degree)
36.5
37

Figure 3.

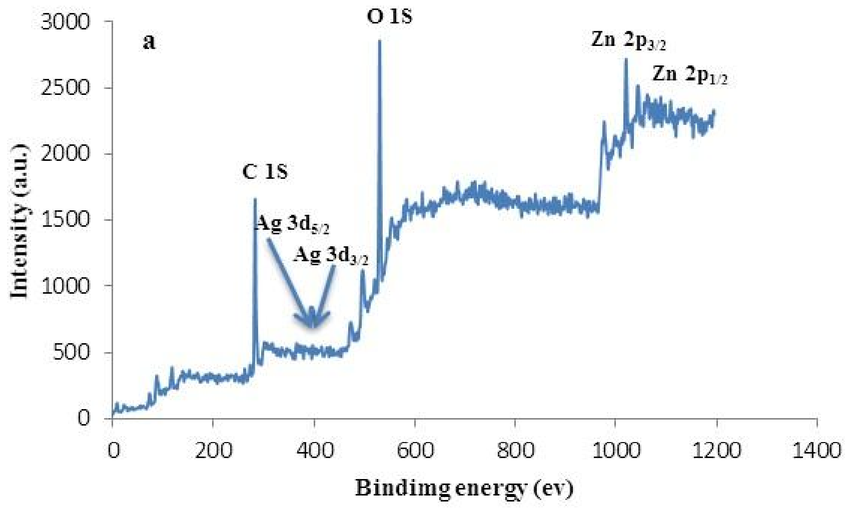
a
O 1S
Zn $2p_{3/2}$
Zn $2p_{1/2}$
C 1S
Ag $3d_{5/2}$
Ag $3d_{3/2}$
3000
2500
2000
1500
1000
500
0
Intensity (a.u.)
0
200
400
600
800
1000
1200
1400
Bindimg energy (ev)

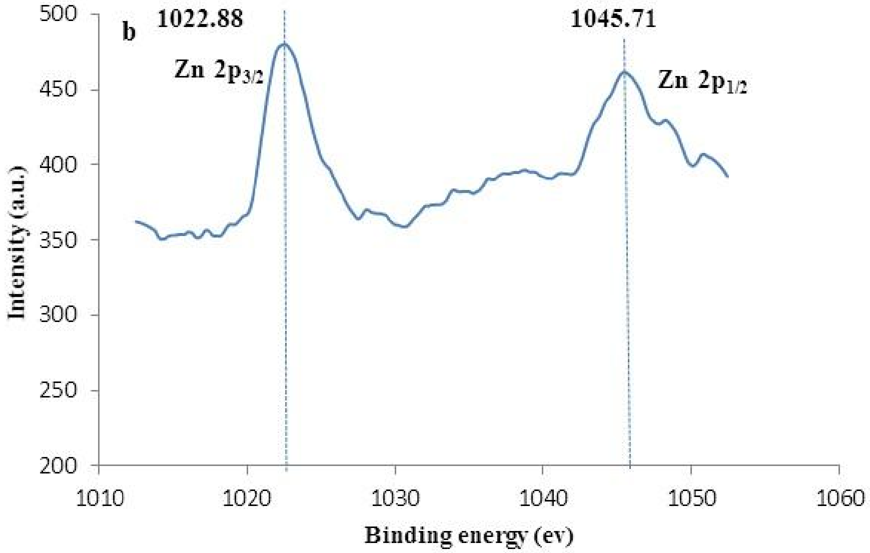
b
1022.88
Zn $2p_{3/2}$
1045.71
Zn $2p_{1/2}$
500
450
400
350
300
250
200
Intensity (a.u.)
1010
1020
1030
1040
1050
1060
Binding energy (ev)

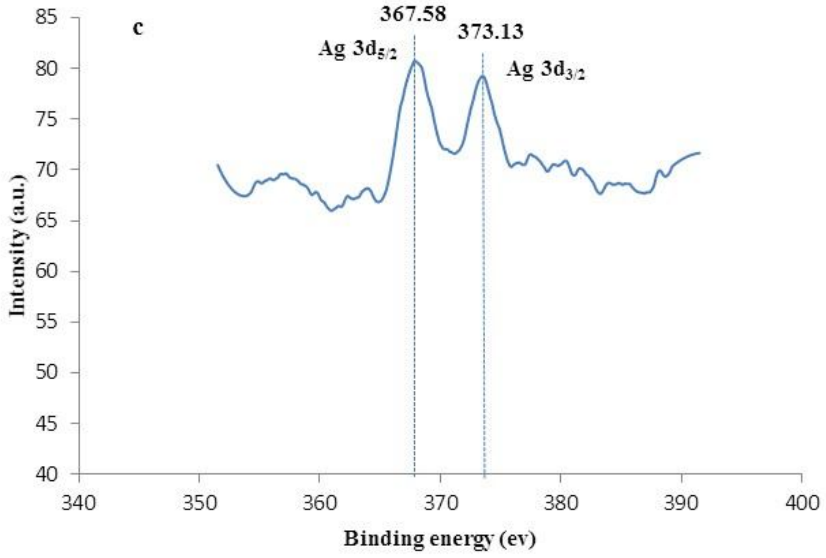
c
367.58
Ag $3d_{5/2}$
373.13
Ag $3d_{3/2}$
85
80
75
70
65
60
55
50
45
40
Intensity (a.u.)
340
350
360
370
380
390
400
Binding energy (ev)

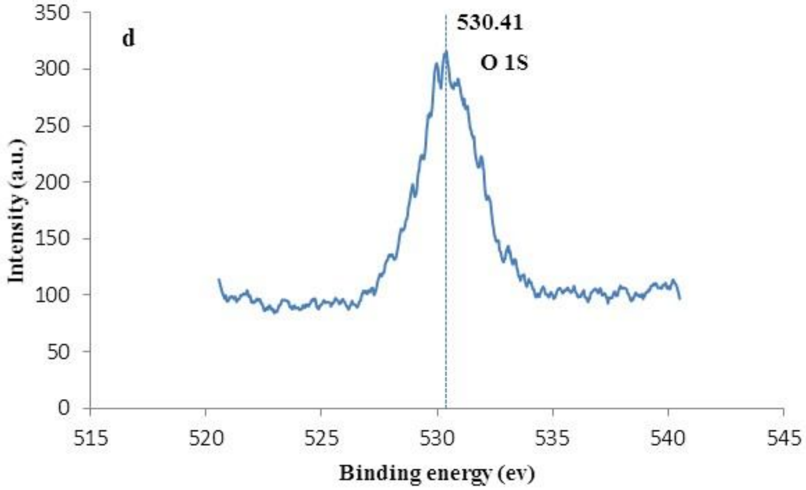
d
530.41
O 1S
Intensity (a.u.)
350
300
250
200
150
100
50
0
515
520
525
530
535
540
545
Binding energy (ev)

Figure 4.

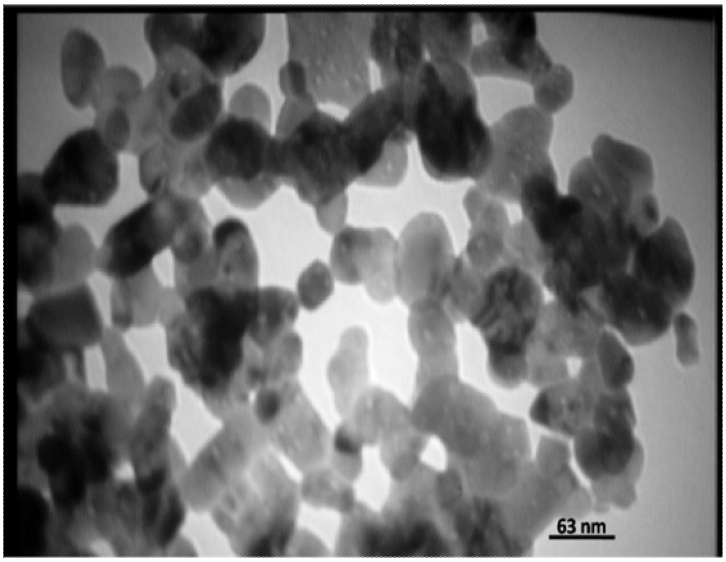

Figure 5.

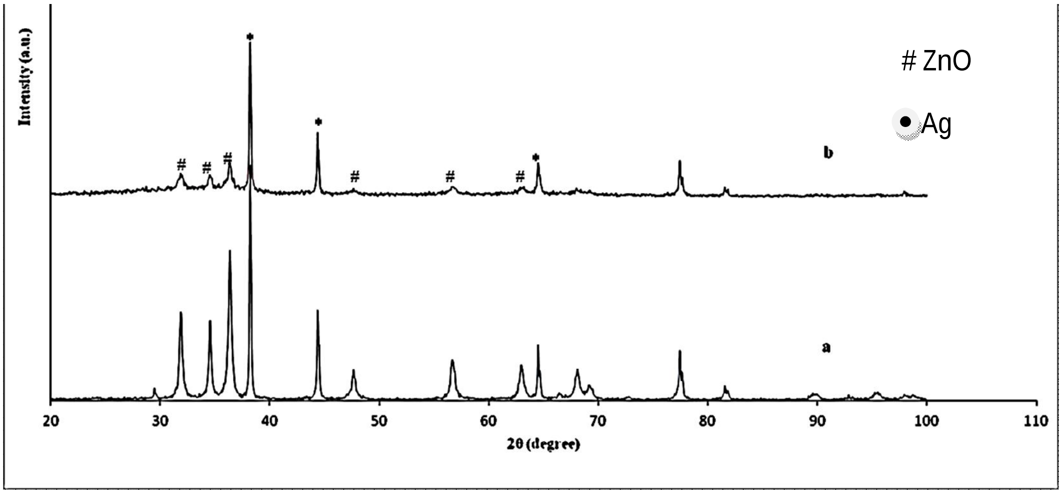

Figure 6.

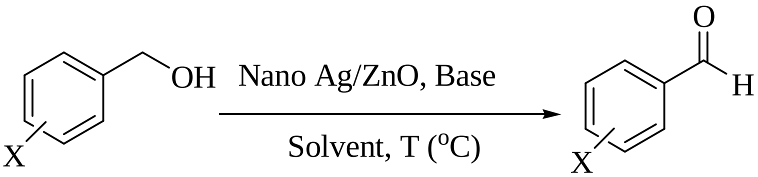

Scheme 1.

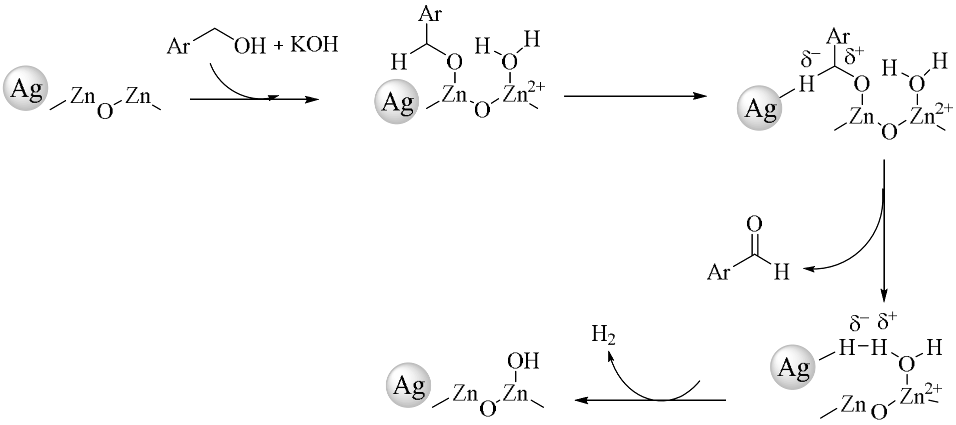

Scheme 2.